THE PROTEIN SOCIETY

Human C3a and C3a desArg anaphylatoxins have conserved structures, in contrast to C5a and C5a desArg

Goran Bajic,[1] Laure Yatime,[1] Andreas Klos,[2] and Gregers Rom Andersen[1]*

[1]Department of Molecular Biology and Genetics, Aarhus University, Gustav Wieds Vej 10C, DK-8000 Aarhus, Denmark
[2]Institut für Medizinische Mikrobiologie und Krankenhaushygiene, Medizinische Hochschule, Carl-Neuberg-Strasse 1, Hannover, Germany

Received 14 September 2012; Revised 8 November 2012; Accepted 13 November 2012
DOI: 10.1002/pro.2200
Published online 26 November 2012 proteinscience.org

Abstract: Complement is a part of innate immunity that has a critical role in the protection against microbial infections, bridges the innate with the adaptive immunity and initiates inflammation. Activation of the complement, by specific recognition of molecular patterns presented by an activator, for example, a pathogen cell, in the classical and lectin pathways or spontaneously in the alternative pathway, leads to the opsonization of the activator and the production of pro-inflammatory molecules such as the C3a anaphylatoxin. The biological function of this anaphylatoxin is regulated by carboxypeptidase B, a plasma protease that cleaves off the C-terminal arginine yielding C3a desArg, an inactive form. While functional assays demonstrate strikingly different physiological effects between C3a and C3a desArg, no structural information is available on the possible conformational differences between the two proteins. Here, we report a novel and simple expression and purification protocol for recombinant human C3a and C3a desArg anaphylatoxins, as well as their crystal structures at 2.3 and 2.6 Å, respectively. Structural analysis revealed no significant conformational differences between the two anaphylatoxins in contrast to what has been reported for C5a and C5a desArg. We compare the structures of different anaphylatoxins and discuss the relevance of their observed conformations to complement activation and binding of the anaphylatoxins to their cognate receptors.

Keywords: complement system; anaphylatoxins; inflammation; C3a; C3a desArg; innate immunity; X-ray structures

Introduction

The human complement system is a key component of innate immunity. It acts as a danger sensing system which participates in the elimination of invading pathogens and cellular debris, initiates inflammation, and bridges the innate and the adaptive immunity,[1–3] Complement is a proteolytic cascade activated through the classical, alternative, and lectin pathways, leading to the enzymatic cleavage of several complement proteins. This cascade not only yields enzymatically active molecules and produces biological effectors, primarily the anaphylatoxins C3a and C5a, the opsonins C3b and C4b but also C5b that can initiate the assembly of a lytic membrane attack complex.[4] C3a and C5a target a

Abbreviations: GPCR, G-protein coupled receptor; IPTG, isopropyl-β-D-thiogalactopyranoside; RMSD, root-mean-square deviation; TEV, tobacco Etch virus; TM, transmembrane.

Additional Supporting Information may be found in the online version of this article.

The coordinates and structure factors for human C3a and C3a desArg are deposited in the RCSB as entries 4HW5 and 4HWJ.

Grant sponsors: DFG-founded CRC587/N16 (Immune reactions of the lung in allergy and infections) and Hallas-Møller (stipend from the Novo-Nordisk Foundation).

*Correspondence to: Gregers Rom Andersen, Department of Molecular Biology and Genetics, Aarhus University, Gustav Wieds Vej 10C, DK-8000 Aarhus, Denmark.
E-mail: gra@mb.au.dk

number of cells including basophils, neutrophils, eosinophils, and mast cells. These anaphylatoxins are potent pro-inflammatory molecules that, by signalling through their cognate GPCRs C3aR and C5aR, trigger oxidative burst,[5,6] chemotaxis, smooth muscle contraction, cellular release of histamine, and increased vascular permeability.[7,8] C3a and C5a have been associated with inflammatory diseases such as ischemia/reperfusion injury,[9] rheumatoid arthritis,[10] and sepsis.[11] Additionally, C3a regulates TNF-α and IL-6 production in monocytes and B cells.[12,13] C3a shares 36% sequence identity with C5a and both proteins are highly basic. The activity of these anaphylatoxins is regulated by carboxypeptidases[14,15] that cleave off the C-terminal arginine, yielding C3a desArg and C5a desArg. C5a desArg retains up to 10% of C5a activity, unlike C3a desArg, which is apparently devoid of any pro-inflammatory activity.[16,17] Interestingly, the third 7TM receptor of the complement system, C5L2, binds C5a and C5a desArg but does not couple to heterotrimeric G-proteins unlike the GPCRs C5aR and C3aR.[8] It has also been suggested that C3a desArg binds to C5L2 and thereby exerts its function as a regulator of triglyceride synthesis rates[18]—although contradicting data exist.[8,19] Thus, in contrast to the canonical GPCR agonists C3a and C5a, the desArg versions might exert other, unrelated functions.

The X-ray structures of plasma-isolated human C3 and C5 as well as bovine C3 have been solved over the last decade, providing insights on how the anaphylatoxin moiety of these complement proteins is folded.[20–22] The three-dimensional structure of recombinant human C5a[23,24] has also been determined by NMR spectroscopy. These structural data all indicate that C3a and C5a adopt an α-helical arrangement and fold into a four-helix bundle motif. In contrast, a recent crystal structure of C5a desArg[25] suggests that the N-terminal α1-helix can detach from the remaining three α-helices. Therefore, C5a and C5a desArg may bind to C5aR and C5L2 in a conformation different from the canonical four-helix bundle.[26]

In the case of C3a, a medium resolution X-ray crystal structure has also been reported already in 1980.[27] However, this structure lacks 14 N-terminal amino-acid residues corresponding roughly to the α1-helix, and the atomic coordinates have never been deposited in the Protein Data Bank. Finally, no structural information is yet available on C3a desArg.

To clarify the conformation of the four helices in C3a and C3a desArg, we have undertaken structural studies of these two human anaphylatoxins. Purification of C3a and C3a desArg from human plasma usually yields preparations that contain a mixture of both proteins, therefore creating a heterogeneity unsuitable for crystallographic studies.[27] Furthermore, the protein is modified by an N-linked glycosylation at the C-terminal end of the α4-helix introducing further flexibility. The production of recombinant C3a and C3a desArg has proven to be challenging and present purification protocols require harsh conditions such as denaturation/renaturation[28] or acidic precipitation,[18] leading to a final protein yield which is rather low. Here, we report the X-ray structures of recombinant, biologically active human C3a and C3a desArg prepared by a fast and simple protocol.

Results

Recombinant C3a and C3a desArg are biologically active

Recombinant human C3a and C3a desArg were expressed in *Escherichia coli* (*E. coli*) cells and purified using a two-step Ni^{2+}-NTA affinity chromatography followed by an ion-exchange chromatography step. C3a and C3a desArg eluted as a single, monodisperse peak on the cation-exchange chromatography column, at respectively 380 and 330 m*M* NaCl, reflecting the difference in their isoelectric properties [Fig. 1(A)]. The final yield of the purification was about 0.5–0.7 mg/L of bacterial culture.

To verify whether our recombinant anaphylatoxins were biologically functional, we performed an *N*-acetyl-β-D-glucosaminidase-release assay on stably transfected cells expressing the anaphylatoxin receptor C3aR, as described previously.[16,29] The curves were compared to those obtained with commercially available C3a purified from human plasma [Fig. 1(B)]. The results show a dose-dependent activation of C3aR-expressing cells. The recombinant and the plasma-purified C3a activate the cells and trigger glucosaminidase release in an almost identical fashion. The measured EC_{50} values are respectively 1.5 ± 0.31 n*M* for recombinant C3a and 1.92 ± 0.35 n*M* for plasma-purified C3a. No cell activation is observed in the case of recombinant C3a desArg even with a 10-fold higher maximum concentration of that used in C3a assays. Three different cell lines were used as controls (mocks, C5aR- and C5L2-expressing cells) and no cell activation was observed (data not shown). These data indicate that the activity and the specificity of recombinant C3a and C3a desArg as measured by glucosaminidase release are identical to those of the proteins purified from human plasma.

C3a and C3a desArg structures

Considering that recombinant C3a but not C3a desArg is able to trigger cell activation, we wanted to investigate if this might be due to conformational differences between the two molecules. For this purpose, we determined the structures of recombinant human C3a and C3a desArg at 2.3 and 2.6 Å resolution, respectively. The two proteins crystallized in a hexagonal space group with almost identical unit

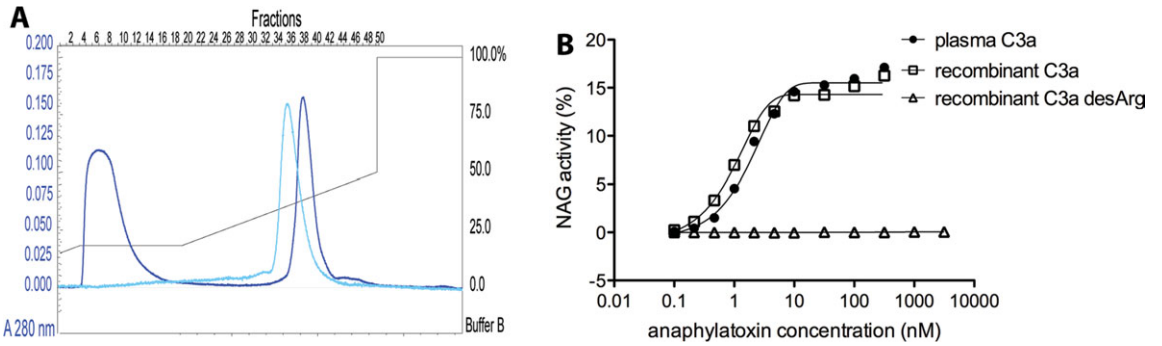

Figure 1. Biological activity of recombinant C3a and C3a desArg. (A) Elution profile of C3a (blue) and C3a desArg (light blue) from the Source 15S column. (B) Comparison of plasma purified and recombinant human C3a and C3a desArg in an *N*-acetyl-β-D-glucosaminidase-release assay performed on stably transfected RBL cells expressing C3aR.

cell parameters (Table I), with however one major difference: the structure of C3a was determined in $P6_3$ with two monomers in the asymmetric unit, whereas C3a desArg crystals possess $P6_322$ symmetry with one monomer in the asymmetric unit. The final models refined to R_{work}/R_{free} values of 24.38/24.27% for C3a ($P6_3$) and 22.28/27.02% for C3a desArg ($P6_322$).

An inspection of the two C3a monomers present in the asymmetric unit suggested that the flexibility of, in particular, the C-terminal Arg748 (prepro-C3 numbering, subtract 671 to obtain residue numbers starting at 1 and ending at 77 for the C3a fragment) violates $P6_322$ symmetry (Supporting Information Fig. S1). This was confirmed by processing the data in higher ($P6_322$) and lower ($P6_3$) symmetry, refining

Table I. *Data Collection and Refinement Statistics*

Protein	C3a	C3a desArg
PDB accession code	4HW5	4HWJ
Space group	$P6_3$	$P6_322$
Crystal data		
Unit cell parameters (Å)	$a = b = 63.89$, $c = 105.19$	$a = b = 63.75$, $c = 106.43$
Solvent content (%)	62	63
No. atoms		
Protein	1261	614
Ligand/ion	10	5
Water	34	22
Data collection		
Resolution range (Å)	19.7–2.3	19.9–2.6
Number of unique reflections	10856 (1295)	4320 (453)
Redundancy	7.6 (7.7)	21.6 (22.2)
Completeness (%)	99.8 (100)	99.6 (100)
R_{sym}[a]	6.6 (76.1)	9.9 (52.1)
R_{meas} (%)[b]	7.1 (82.1)	10.1 (53.3)
Mean $I/\sigma(I)$	20.6 (3.5)	29.3 (8.3)
Overall Wilson B-factor (Å^2)[c]	51.3	41.1
Refinement		
Resolution range	19.7–2.3	19.9–2.6
Reflections	11591	4338
R factor	0.2438	0.2228
Free R factor	0.2427	0.2702
Deviations from ideal values		
RMSD bond length (Å)	0.007	0.002
RMSD bond angles (°)	1.034	0.629
Average B factor (Å^2)	66.0	49.3
Ramachandran favored (%)[d]	94.0	98.6
Ramachandran outliers (%)[d]	1.33	0

[a] $R_{sym} = \frac{\sum_h \left| \hat{I}_h - I_{h,i} \right|}{\sum_h \sum_i^{n_h} I_{h,i}}$ with $\hat{I}_h = \frac{1}{n_h} \sum_i^{n_h} I_{h,i}$.

[b] $R_{meas} = \frac{\sum_h \sqrt{\frac{n_h}{n_h - 1}} \sum_i^{n_h} \left| \hat{I}_h - I_{h,i} \right|}{\sum_h \sum_i^{n_h} I_{h,i}}$ with $\hat{I}_h = \frac{1}{n_h} \sum_i^{n_h} I_{h,i}$.

[c] As reported by XDS.

[d] As reported by MolProbity.

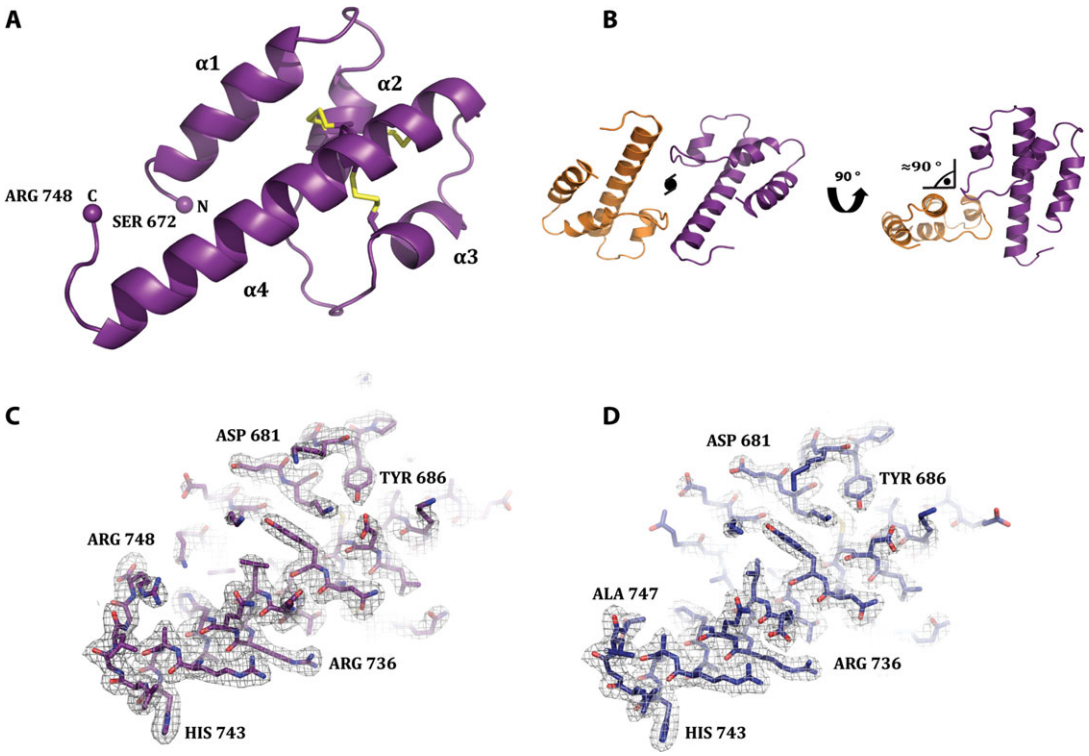

Figure 2. General overview of the anaphylatoxins structures. (A) Overall structure of human C3a at 2.3 Å resolution. The N- and C-terminal residues are indicated. The four alpha helices are numbered. The three disulfide bridges stabilizing the four-helix bundle are shown in yellow sticks. (B) Structure of the two C3a molecules present in the asymmetric unit and related by noncrystallographic twofold symmetry. (C and D) $2mF_o$-DF_c electron density maps, contoured at 1σ for C3a (panel C) and C3a desArg (panel D), respectively. The C3a and C3a desArg molecules are oriented as in panel A.

and monitoring the R factors. In fact, the data processed in $P6_322$ had higher R_{sym} values and the C3a model was refined to a higher R_{free} value compared to $P6_3$. The fact that C3a desArg, lacking the Arg 748, refines well in $P6_322$ further corroborates the pseudosymmetry in the case of C3a.

The overall structural arrangement of C3a is shown in Figure 2A. Both anaphylatoxins adopt the characteristic four-helix bundle fold with residues 675–684 (4–13 in C3a numbering) forming the α1-helix, residues 691–697 (20–26) form the α2-helix, residues 707–711 (36–40) comprises the α3-helix, and residues 718–743 (47–72) form the α4-helix. Although only helices α2, α3, and α4 were observed in the original crystal structure of C3a,[27] a four helical bundle structure of C3a was earlier suggested based on NMR data[30] and comparison with C5a.[31] The packing of the four antiparallel helices is primarily stabilized by three disulfide bridges: Cys693-Cys720 (α2-α4), Cys694-Cys727 (α2-α4), and Cys707-Cys728 (α3-α4). There are no indications of an alternative disulfide bridge pattern observed upon reduction and denaturation of C3a,[32] and in fact the cysteine sulfur positions are so well-defined that they have been very recently used for Radiation-damage-induced-phasing.[33] Clear and well-defined electron density was visible for most of the C3a and C3a desArg molecules [Figs. 2(C,D)], except for Arg748 in the C3a structure, as mentioned above. The loop region between helices α3 and α4, encompassing residues 713–719, was also more poorly defined in the electron density maps suggesting flexibility of this region. The final models contain residues 672–748 for C3a and residues 673–747 for C3a desArg.

The two monomers present in the asymmetric unit of the C3a crystal are arranged in an antiparallel, practically perpendicular fashion around the noncrystallographic twofold axis [Fig. 2(B)]. The reported structure of C5a desArg likewise showed a dimeric organization of the asymmetric unit and the observed dimer has been proposed to be of functional relevance for the binding of C5a/C5a desArg to the C5aR/C5L2 receptors. However, the existence of this dimer in a physiological setting remains unproven. Analysis with PISA[34] of the dimer contained in the asymmetric unit of our C3a crystal suggests that this dimer is unlikely to be of biological relevance.

Superimposition of C3a and C3a desArg [Fig. 3(A)] reveals a high similarity between the two structures with an RMSD of 0.40 Å on Cα atoms. Apart from the C-terminal arginine, the most pronounced difference between the two structures can be observed for the mobile loop region between helices α3 and α4 (residues 713–719). C3a and C3a desArg are highly cationic molecules possessing

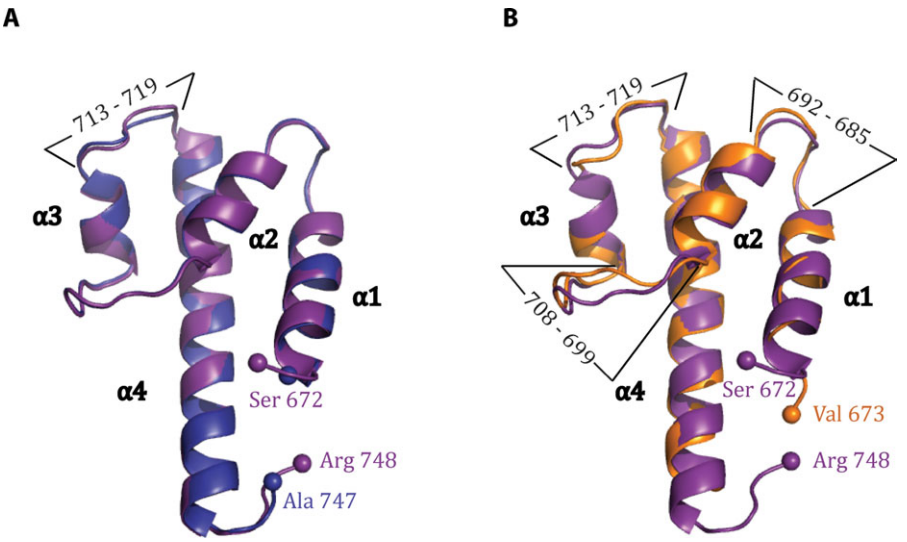

Figure 3. Comparison of the free and C3-bound anaphylatoxins structures (A) Superimposition of the C3a (violet) and C3a desArg (blue) structures determined in this study. The regions displaying the most significant structural differences are labeled with residue numbers. (B) Superimposition of the recombinant C3a (violet, this study) and the C3a moiety from the human C3 (orange, PDB ID 2A73 [20]). The regions displaying the most significant structural differences are indicated by black lines and labeled with residue numbers.

seven lysine and 12 or 11 arginine residues respectively. In the unbound anaphylatoxins these residues form a large, positively charged solvent-accessible surface area most likely important for interaction with negatively charged elements located on the extracellular face of C3aR such as the sulfotyrosine region.[35] However, this positively charged patch is partially shielded in the intact C3 (Supporting Information Fig. S2) thereby effectively preventing interaction of the highly abundant C3 with, for example, C3aR.

Comparison of recombinant C3a/C3a desArg with the C3a moiety of human and bovine C3

The X-ray crystal structures of both bovine and human C3 have been determined.[20,21] Structural superimposition indicates a very similar conformation of C3a and C3a desArg in comparison to their equivalent parts in the complete bovine and human C3 molecules. The average RMSD of recombinant C3a and C3a desArg superimposed to human C3 residues 651–719 are 1.19 and 1.21 Å, respectively, with the major discrepancies occurring in the loop regions. One major difference is at the C-terminus, but this is to be expected as this region is part of a mobile loop region in C3, whereas it terminates with a free C-terminal carboxyl group in the anaphylatoxins. Comparison of our structures of human C3a and C3a desArg to the C3a moiety of bovine C3 [Fig. 3(B)] resulted in similar observations with noticeable differences in the loop regions as well as the N- and C-terminal regions. The average RMSD on Cα atoms is 1.24 Å for C3a and 1.23 Å for C3a desArg as compared to the C3a moiety of bovine C3. In conclusion, the release of C3a from C3 upon convertase cleavage does not impose large conformational rearrangements in C3a.

Comparison to other anaphylatoxins

Human anaphylatoxins C3a, C4a and C5a share approximately 18% of sequence identity and they all possess the three disulfide bridges that interlock the α2, α3, and α4 helices. We have recently determined the structures of unbound C4 and of C4 in complex with a fragment of the MASP-2 proteinase cleaving C4 in the lectin pathway of complement activation.[36] In the unbound C4 structure, the density for helix α1 is poorly defined, suggesting a high mobility of this helix. By contrast, α1 becomes ordered and integrated in the four-helix bundle in the C4·MASP-2 complex [Fig. 4(A)]. As mentioned above, the crystal structure of C5a desArg[25] displays a protein folding into a three-helix bundle and contains two nonidentical monomers in the asymmetric unit. One forms a regular three-helix bundle, where the α1 and α2 helices have merged to form a single long helix. In the other monomer, the α1-helix is protruding at an angle of almost 120° from the α2-helix. Structural superimposition of C5a with the two unequal monomers of C5a desArg [Fig. 4(B)] highlights these conformational differences. In all structures of intact C5,[22,37,38] the C5a moiety adopts a classical four-helix bundle, but the three-helix bundle conformation may be present in pro-C5 for topological reasons.[25]

Analysis of the interaction forces of the N-terminal α1-helix in C3a reveals that packing of α1 against the remaining three helices is mediated by five hydrogen bonds, a salt bridge formed with α4,

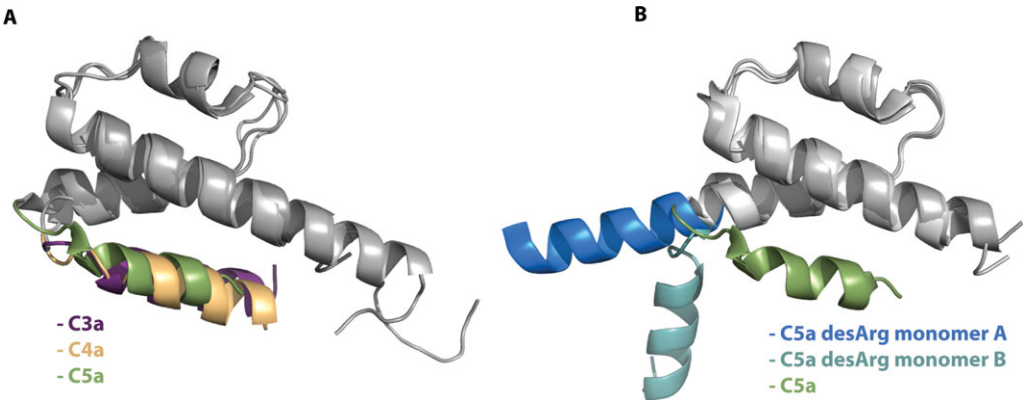

Figure 4. Comparison of C3a and C3a desArg with other anaphylatoxins. (A) Superimposition of the four-helix bundle fold of the recombinant human C3a (violet, this study), of the C4a moiety from the human C4 (yellow, PDB ID 4FXG[32]) and of the C5a moiety from the human C5 (green, PDB ID 3CU7[22]). (B) Superimposition of the four-helix-bundle from the C5a moiety of the human C5 (green, PDB ID 3CU7[22]) and from the two monomers of the human C5a desArg (blue, PDB ID 3HQA and cyan, PDB ID 3HQB[25]), present in the asymmetric unit of the crystal structure, showing the α1-helix swing-out motion of C5a desArg.

and a salt bridge formed with α2 [Fig. 5(A)]. In contrast, most of the residues found at the interface between α1 and α4 in the C5a structure[22] are nonpolar and no hydrogen bonds are observed [Fig. 5(B)]. This suggests that the packing into a four-helix bundle motif might be less stable in the case of C5a, which might explain the tendency for α1 to be more mobile. Conversely, the flexibility of helix α1 observed in the C4 structure suggests that this property is not unique to C5a.

Discussion

Here, we have reported a new and simple protocol for the purification of recombinant C3a and C3a desArg anaphylatoxins expressed in bacteria. Contrary to previously reported protocols, our procedure is straightforward, fast, and yields reasonable quantities of pure crystallizable protein. Our recombinant C3a is able to induce glucosaminidase release from C3aR expressing cells, showing that the recombinant anaphylatoxin has the classical biological activity associated with it, whereas C3a desArg is unable to trigger release as expected despite their almost identical structures. These data indicate that the activity and the specificity (mediated by the C3aR) of our recombinant C3a and C3a desArg as measured by glucosaminidase release are identical to those of the proteins purified from human plasma. Whether our recombinant anaphylatoxins are active in other functions ascribed to them such as antimicrobial activity,[39] binding to C5L2 and regulation of triglyceride synthesis[18] remains to be proven. We have further crystallized and solved the structures of both proteins at 2.3 and 2.6 Å resolution, respectively. Our structures demonstrate that the overall conformation of C3a and C3a desArg is almost identical and that both proteins adopt a canonical four-helix bundle fold. The secondary structure we observe is somewhat at variance with an NMR study of C3a-desArg where the α4-helix was found to extend to Gln738, the last six residues were in dynamic random coil conformation, and the α1-helix to begin at Arg679[30] suggesting that crystal packing may stabilize the ends of helices α1 and α4.

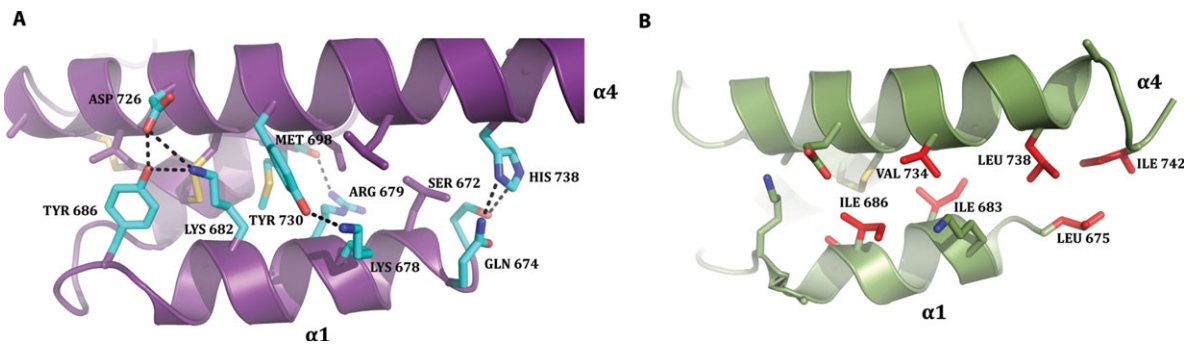

Figure 5. Comparison of the interactions stabilizing α1-helix packing within the four-helix bundle for the recombinant human C3a (A) and the human C5a as part of C5 (PDB ID 3CU7[22]) (B). The residues involved in hydrogen bond and salt bridge (dotted lines) formation are highlighted in cyan in the C3a structure, and hydrophobic residues at the α1-α4 helix interface are shown in red in the C5a structure.

In contrast to the stable four-helix bundle observed in C3a and C3a desArg a high degree of flexibility is observed for the N-terminal helix of C5a desArg.[25] However, this behavior has not been observed in NMR studies of C5a[23,24,40] suggesting that crystallization may have promoted the release of the α1-helix in the C5a desArg. Conversely, the flexibility observed for the α1-helix of the C4a moiety within C4 shows that this movement might be possible for other anaphylatoxins. It is also possible that the extended conformation of the α1-helix exists in the proform of all three complement proteins C3, C4, and C5, as earlier suggested,[25] and that the four-helix bundle is formed in C3 and C5 once the proteins maturate by proteolytic processing, whereas both conformations seem to exist in C4.

Another possibility is that the swing-out movement of helix α1 observed in C5a desArg only occurs in the presence of an interaction partner such as the C5aR/C5L2 receptors and the carboxypeptidases. In the case of C3a and C3a desArg, we do not observe any significant structural differences even though the physiological effects of the two molecules are strikingly different. The sole influence of the C-terminal arginine residue could therefore account for the difference in their biological properties. However, one cannot exclude that conformational differences between the two molecules may occur upon binding to their cognate receptor C3aR.[16] To answer these important questions, detailed structural information concerning complexes between anaphylatoxins and their receptors must be obtained.

Materials and Methods

Genes and plasmids

The codon-optimized C3a gene, flanked by BamHI and HindIII restriction sites and containing a 5′ insertion corresponding to TEV protease cleavage site, was purchased from GenScript. An additional four amino-acid linker (GAAG) was introduced between the TEV cleavage site and the beginning of C3a sequence using the QuikChange site-directed mutagenesis kit (Stratagene). The C3a desArg construct was generated from the C3a construct. The genes were subsequently cloned into pET32a vector (Novagen). The recombinant vector was used for transformation of Shuffle T7 electrocompetent *E. coli* cells (New England Biolabs).

Overexpression and purification

E. coli cells harbouring the plasmid were grown at 37°C in 2xTY medium supplemented with 100 μg/mL of ampicillin to an $OD_{600} \approx 0.6$. Protein expression was induced with 1 m*M* IPTG and the cultures were grown over night at 18°C and cells were harvested by centrifugation (7000*g* for 20 min at 4°C). Cell pellets were resuspended in 50 m*M* HEPES pH 8, 300 m*M* NaCl, 30 m*M* imidazole, 1 m*M* PMSF (binding buffer). Cells were disrupted by sonication, and cellular debris removed by centrifugation (20,000*g* for 30 min at 4°C). The resulting supernatant was loaded on a HisTrap FF crude column (GE Healthcare) and the column was washed with three volumes of binding buffer and five volumes of binding buffer supplemented with 1*M* NaCl. The recombinant protein was eluted in 20 mL of 50 m*M* HEPES pH 8, 300 m*M* NaCl, 500 m*M* imidazole. House-made recombinant TEV protease was added in a ratio of 1:50 (w/w), and digestion was conducted in a dialysis bag (3500 Da cut-off) over night at 4°C against 2 L of 50 m*M* HEPES pH 8, 300 m*M* NaCl, 0.5 m*M* EDTA. The resulting cleavage product was loaded on the HisTrap column and the untagged C3a or C3a desArg was eluted in the flow-through. Finally, the protein was purified by ion-exchange chromatography (Source 15S 9 mL, GE Healthcare) in 50 m*M* HEPES pH 8 and eluted using a linear NaCl gradient from 150 to 500 m*M*. Fractions containing the recombinant protein were pooled, concentrated and stored at −80°C. Prior to the use in a cell-based functional assay, the samples were purified on a Detoxi-Gel™ prepacked column (Thermo Scientific) for endotoxin removal.

N-acetyl-β-D-glucosaminidase-release assay (GARA)

The release of the lysosomal enzyme *N*-acetyl-β-D-glucosaminidase was assayed as described.[16,29] Briefly, stably transfected RBL cells (a rat basophil cell line) were harvested, resuspended in HAG-CM-complete buffer (20 m*M* HEPES pH 7.4, 125 m*M* NaCl, 5 m*M* KCl, 1 m*M* $CaCl_2$, 1 m*M* $MgCl_2$, 0.5 m*M* glucose, 0.25% BSA) at a concentration of 2×10^6 cells/ml and incubated at 37°C for 20 min. In parallel, anaphylatoxin dilutions, supplemented with 1 m*M* of cytochalasin B, were incubated at 37°C. The cells were added to the anaphylatoxin dilutions and incubated for 3 min at 37°C. The samples were subsequently transferred to ice and centrifuged at 400*g* for 3 min at 4°C. NAG activity was assessed by incubating the supernatant in the presence of 4.57 m*M* p-Nitrophenyl-*N*-acetyl-beta-D-glucosamide (Sigma) for 60 min at 37°C. Enzymatic reactions were quenched by addition of 0.4*M* glycine-NaOH (pH 10.4) and spectral absorbance was measured at 405 nm. The maximum NAG release (i.e., 100% lysis in the graph) was determined with 1% Triton X-100. EC_{50} values are means ± standard deviation of multiple independent experiments.

Crystallization and data collection

Crystallization experiments were performed by vapour diffusion at 19°C. The protein sample (1 μL at 16 mg/mL in 25 mM HEPES pH 8, 150 m*M*

NaCl) was mixed with an equal volume of reservoir solution. C3a crystallized in 2–2.2*M* ammonium sulfate, with a pH ranging from 6 to 9 and C3a desArg crystallized in 0.2*M* ammonium sulfate, 0.1*M* Tris pH 7.5–8.5, 25% (w/v) PEG 3350. For data collection, the crystals were cryo-protected in the reservoir buffer supplemented with 25% sucrose before flash cooling into liquid nitrogen. Data were collected at beamline I911-3 at MAX-lab in Lund, Sweden. An initial dataset collected for C3a on beamline ID23-2 at ESRF was used to implement a RIP-phasing method based on the cleavage of disulfide bridges induced by radiation damage during data collection.[33]

Structure determination

All datasets were processed with XDS.[41] Both structures were solved by molecular replacement in PHASER,[42] using the C3a moiety of human C3 (PDB ID 2A73[20]) as search model. Models were rebuild in COOT[43] and refined with PHENIX.REFINE[44] using individual ADP as well as TLS refinement. After the first rounds of refinement, it became evident that the refinement of the C3a structure in space group $P6_322$ was stuck at high R-factor values as compared to the C3a desArg structure. The C3a dataset was therefore reprocessed in the lower symmetry space groups $P6_3$ and P321. Refinement for C3a was finally carried out in $P6_3$. The quality of the final models was assessed with *MOLPROBITY*[45] and figures were made with PyMOL (Schrödinger LLC).

Acknowledgments

The authors thank Maike Bublitz and the beamline staffs at Max-Lab and ESRF for help during data collection and Claudia Rheinheimer for excellent technical assistance. We thank the Lundbeck Foundation for supporting this work through the grant: Lundbeck Foundation Nanomedicine Center for Individualized Management of Tissue Damage and Regeneration.

References

1. Carroll MC (2004) The complement system in regulation of adaptive immunity. Nat Immunol 5:981–986.
2. Guo RF, Ward PA (2005) Role of C5a in inflammatory responses. Annu Rev Immunol 23:821–852.
3. Hawlisch H, Kohl J (2006) Complement and Toll-like receptors: key regulators of adaptive immune responses. Mol Immunol 43:13–21.
4. Kolb WP, Haxby JA, Arroyave CM, Muller-Eberhard HJ (1972) Molecular analysis of the membrane attack mechanism of complement. J Exp Med 135:549–566.
5. Elsner J, Oppermann M, Czech W, Dobos G, Schopf E, Norgauer J, Kapp A (1994) C3a activates reactive oxygen radical species production and intracellular calcium transients in human eosinophils. Eur J Immunol 24:518–522.
6. Elsner J, Oppermann M, Czech W, Kapp A (1994) C3a activates the respiratory burst in human polymorphonuclear neutrophilic leukocytes via pertussis toxin-sensitive G-proteins. Blood 83:3324–3331.
7. Hugli TE (1990) Structure and function of C3a anaphylatoxin. Curr Top Microbiol Immunol 153:181–208.
8. Klos A, Tenner AJ, Johswich KO, Ager RR, Reis ES, Kohl J (2009) The role of the anaphylatoxins in health and disease. Mol Immunol 46:2753–2766.
9. Arumugam TV, Shiels IA, Woodruff TM, Granger DN, Taylor SM (2004) The role of the complement system in ischemia-reperfusion injury. Shock 21:401–409.
10. Linton SM, Morgan BP (1999) Complement activation and inhibition in experimental models of arthritis. Mol Immunol 36:905–914.
11. Ward PA (2008) Role of the complement in experimental sepsis. J Leukoc Biol 83:467–470.
12. Fischer WH, Hugli TE (1997) Regulation of B cell functions by C3a and C3a(desArg): suppression of TNF-alpha, IL-6, and the polyclonal immune response. J Immunol 159:4279–4286.
13. Fischer WH, Jagels MA, Hugli TE (1999) Regulation of IL-6 synthesis in human peripheral blood mononuclear cells by C3a and C3a(desArg). J Immunol 162:453–459.
14. Bokisch VA, Muller-Eberhard HJ (1970) Anaphylatoxin inactivator of human plasma: its isolation and characterization as a carboxypeptidase. J Clin Invest 49: 2427–2436.
15. Matthews KW, Mueller-Ortiz SL, Wetsel RA (2004) Carboxypeptidase N: a pleiotropic regulator of inflammation. Mol Immunol 40:785–793.
16. Wilken HC, Gotze O, Werfel T, Zwirner J (1999) C3a(desArg) does not bind to and signal through the human C3a receptor. Immunol Lett 67:141–145.
17. Sayah S, Jauneau AC, Patte C, Tonon MC, Vaudry H, Fontaine M (2003) Two different transduction pathways are activated by C3a and C5a anaphylatoxins on astrocytes. Brain Res Mol Brain Res 112:53–60.
18. Cui W, Lapointe M, Gauvreau D, Kalant D, Cianflone K (2009) Recombinant C3adesArg/acylation stimulating protein (ASP) is highly bioactive: a critical evaluation of C5L2 binding and 3T3–L1 adipocyte activation. Mol Immunol 46:3207–3217.
19. Johswich K, Martin M, Thalmann J, Rheinheimer C, Monk PN, Klos A (2006) Ligand specificity of the anaphylatoxin C5L2 receptor and its regulation on myeloid and epithelial cell lines. J Biol Chem 281:39088–39095.
20. Janssen BJ, Huizinga EG, Raaijmakers HC, Roos A, Daha MR, Nilsson-Ekdahl K, Nilsson B, Gros P (2005) Structures of complement component C3 provide insights into the function and evolution of immunity. Nature 437:505–511.
21. Fredslund F, Jenner L, Husted LB, Nyborg J, Andersen GR, Sottrup-Jensen L (2006) The structure of bovine complement component 3 reveals the basis for thioester function. J Mol Biol 361:115–127.
22. Fredslund F, Laursen NS, Roversi P, Jenner L, Oliveira CL, Pedersen JS, Nunn MA, Lea SM, Discipio R, Sottrup-Jensen L, Andersen GR (2008) Structure of and influence of a tick complement inhibitor on human complement component 5. Nat Immunol 9:753–760.
23. Zuiderweg ER, Nettesheim DG, Mollison KW, Carter GW (1989) Tertiary structure of human complement component C5a in solution from nuclear magnetic resonance data. Biochemistry 28:172–185.
24. Zhang X, Boyar W, Toth MJ, Wennogle L, Gonnella NC (1997) Structural definition of the C5a C terminus by two-dimensional nuclear magnetic resonance spectroscopy. Proteins 28:261–267.

25. Cook WJ, Galakatos N, Boyar WC, Walter RL, Ealick SE (2010) Structure of human desArg-C5a. Acta Crystallogr D Biol Crystallogr 66:190–197.
26. Laursen NS, Magnani F, Gottfredsen RH, Petersen SV, Andersen GR (2012) Structure, function and control of complement C5 and its proteolytic fragments. Curr Mol Med 12:1083–1097.
27. Huber R, Scholze H, Paques EP, Deisenhofer J (1980) Crystal structure analysis and molecular model of human C3a anaphylatoxin. Hoppe Seylers Z Physiol Chem 361:1389–1399.
28. Fukuoka Y, Yasui A, Tachibana T (1991) Active recombinant C3a of human anaphylatoxin produced in Escherichia coli. Biochem Biophys Res Commun 175: 1131–1138.
29. Gerard NP, Gerard C (1990) Construction and expression of a novel recombinant anaphylatoxin, C5a-N19, as a probe for the human C5a receptor. Biochemistry 29:9274–9281.
30. Nettesheim DG, Edalji RP, Mollison KW, Greer J, Zuiderweg ER (1988) Secondary structure of complement component C3a anaphylatoxin in solution as determined by NMR spectroscopy: differences between crystal and solution conformations. Proc Natl Acad Sci USA 85:5036–5040.
31. Morikis D, Holland MCH, Lambris JD. Structure of the anaphylatoxins C3a and C5a. In: Morikis D, Lambris JD, Eds. (2005) Structural biology of the complement system. Boca Raton: CRC press, pp 161–177.
32. Chang JY, Lin CC, Salamanca S, Pangburn MK, Wetsel RA (2008) Denaturation and unfolding of human anaphylatoxin C3a: an unusually low covalent stability of its native disulfide bonds. Arch Biochem Biophys 480:104–110.
33. de Sanctis D, Nanao MH (2012) Segmenting data sets for RIP. Acta Crystallogr D Biol Crystallogr 68: 1152–1162.
34. Krissinel E, Henrick K (2007) Inference of macromolecular assemblies from crystalline state. J Mol Biol 372: 774–797.
35. Gao J, Choe H, Bota D, Wright PL, Gerard C, Gerard NP (2003) Sulfation of tyrosine 174 in the human C3a receptor is essential for binding of C3a anaphylatoxin. J Biol Chem 278:37902–37908.
36. Kidmose TR, Laursen SN, Dobó J, Kjaer RT, Sirotkina S, Yatime L, Sottrup-Jensen L, Thiel S, Gál P, Andersen GR (2012) Structural basis for activation of the complement system by C4 cleavage. Proc Natl Acad Sci USA 109:15425–15430.
37. Laursen NS, Gordon N, Hermans S, Lorenz N, Jackson N, Wines B, Spillner E, Christensen JB, Jensen M, Fredslund F, Bjerre M, Sottrup-Jensen L, Fraser JD, Andersen GR (2010) Structural basis for inhibition of complement C5 by the SSL7 protein from Staphylococcus aureus. Proc Natl Acad Sci USA 107:3681–3686.
38. Laursen NS, Andersen KR, Braren I, Spillner E, Sottrup-Jensen L, Andersen GR (2011) Substrate recognition by complement convertases revealed in the C5-cobra venom factor complex. EMBO J 30:606–616.
39. Nordahl EA, Rydengard V, Nyberg P, Nitsche DP, Morgelin M, Malmsten M, Bjorck L, Schmidtchen A (2004) Activation of the complement system generates antibacterial peptides. Proc Natl Acad Sci USA 101: 16879–16884.
40. Zuiderweg ER, Fesik SW (1989) Heteronuclear three-dimensional NMR spectroscopy of the inflammatory protein C5a. Biochemistry 28:2387–2391.
41. Kabsch W (2010) Xds. Acta Crystallogr D Biol Crystallogr 66:125–132.
42. McCoy AJ, Grosse-Kunstleve RW, Adams PD, Winn MD, Storoni LC, Read RJ (2007) Phaser crystallographic software. J Appl Crystallogr 40:658–674.
43. Emsley P, Cowtan K (2004) Coot: model-building tools for molecular graphics. Acta Crystallogr D Biol Crystallogr 60:2126–2132.
44. Adams PD, Afonine PV, Bunkoczi G, Chen VB, Davis IW, Echols N, Headd JJ, Hung LW, Kapral GJ, Grosse-Kunstleve RW, McCoy AJ, Moriarty NW, Oeffner R, Read RJ, Richardson DC, Richardson JS, Terwilliger TC, Zwart PH (2010) PHENIX: a comprehensive Python-based system for macromolecular structure solution. Acta Crystallogr D Biol Crystallogr 66:213–221.
45. Davis IW, Leaver-Fay A, Chen VB, Block JN, Kapral GJ, Wang X, Murray LW, Arendall WB, 3rd, Snoeyink J, Richardson JS, Richardson DC (2007) MolProbity: all-atom contacts and structure validation for proteins and nucleic acids. Nucleic Acids Res 35:W375–W383.